

# Modelling the wind response of large bridges by use of the finite element method

Alberto PATRON  
Christian CRÉMONA

Laboratoire Central des Ponts et Chaussées

179

## INTRODUCTION

Thanks to improvements in computation methods, materials and construction techniques, cable bridges have been revolutionized over the recent past to an extent never before experienced. This evolution has been accompanied by an increase in span lengths, thus implying greater flexibility along with higher risk with respect to dynamic effects. Only after the spectacular collapse of the Tacoma Bridge in the United States in 1940 did such dynamic effects produced by wind on large bridges actually start to be examined with greater emphasis.

The initial research focused on studying stability as regards *aeroelastic phenomena*. These effects arise on a flexible structure whenever displacements and aerodynamic forces interact. Highly complex phenomena take place as the oscillating structure disturbs airflow and, consequently, forces generated act upon the structure itself. This type of problem has been examined since the 1920's in the field of aeronautics. Several analytical formulations have been proposed in this same context. Unfortunately, as opposed to airfoils, bridge deck cross-sections are *poorly-profiled structures*, which prevents against any direct application of such theories. The work of Bleich [1], Bisplinghoff [2] and Scanlan [3] in particular enabled establishing the set of models describing aeroelastic forces for bridge decks. The fundamental difference inherent in these models, as compared with those from aeronautics, stems from the fact that they rely heavily on experimental parameters of the cross-section of the bridge deck.

During the 1960's, the dynamic response of structures submitted to wind turbulence began receiving attention, via the theory of random vibrations. Initial applications of this theory to the study of flexible bridges submitted to wind are owed to Davenport [4], whose approach consisted of analyzing the turbulence effect (as characterized by its spectral density function) like a stochastic loading that excites the structure, which is typically considered as having so-called "classical" damping. This hypothesis serves to decouple the movement equations (by using the undamped eigenmodes basis)

into a set of independent modal equations. It then becomes possible to separately evaluate the spectral power density and the standard deviation of the response of each mode. These two problem situations (stability study and turbulence response evaluation) were thus treated independently and the interaction between both phenomena had for a long time been neglected.

In current practice, the study of wind dynamic effects on bridges is divided into two parts: aeroelastic stability verification, and evaluation of structural response under the turbulent wind effect. The aeroelastic behaviour of the fluid-structure system is evaluated thanks to wind tunnel tests and, if necessary, the bridge cross-section is profiled in order to ensure aeroelastic stability prior to assessing the turbulent wind response. The influence of aeroelastic forces on the turbulence response is considered in a simplified way by introducing a so-called "aerodynamic damping" superimposed upon the damping of each mode [5]. In most structures, modal equations are coupled by damping terms and, in the case of large bridges in airflow, by aeroelastic terms. From a general point of view, aeroelastic effects may be interpreted as corrective terms for bridge damping and stiffness. The dynamic characteristics are thereby modified: oscillation frequencies and modal shapes are both "aeroelastically-modified". Modal superposition using classical eigenmodes would thus no longer be possible herein.

Over the past twenty years, many methods have been proposed in order to add realism when considering fluid-structure interaction effects in the response to turbulence, either over the frequency domain [6-8] or over the time domain [9,10]. The work presented in this article constitutes an extension to this past research and makes use of the capacities offered by current computing resources. A general and comprehensive approach is thus proposed herein for studying the temporal and spectral dynamic responses of flexible bridges submitted to wind turbulence by incorporating aeroelastic forces. The first part of this article will focus on describing and mathematically modelling the forces generated by turbulent airflow on a bridge deck. Special emphasis will be placed on the forces produced by turbulence and aeroelastic forces, for which formulations within both the temporal and frequency domains are given. The second part is devoted to a numerical evaluation of the wind response of flexible bridges. The set of dynamic equations of the coupled fluid-structure system will be established. Next, verification of the structural stability will be presented by introducing a method for determining critical flutter wind speeds. The turbulence response will then be introduced via two approaches: the first consists of performing a pure-frequency computation of the "aeroelastically-coupled" system of modal equations, while the second solves system dynamic equations over the time domain.

The numerical implementation of these developments has been conducted through the EOLE module of the CESAR-LCPC finite element method program. In order to illustrate the various aspects associated with the proposed approach, the results obtained from finite element computations on the Vasco de Gama Bridge (Lisbon, Portugal) will be discussed in a third part of this article.

## FORCES GENERATED BY TURBULENT WIND ON A BRIDGE DECK

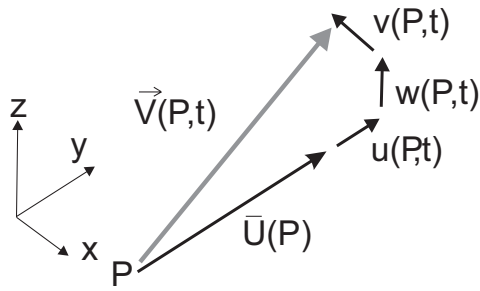
### Modelling turbulent wind

Turbulent wind speed is classically modeled as the superposition of an average term and a fluctuating term. Within a Cartesian coordinate system (Ox,Oy,Oz) with the x-axis lying parallel to the prevailing wind direction, the speed at point P in space can then be written as follows:

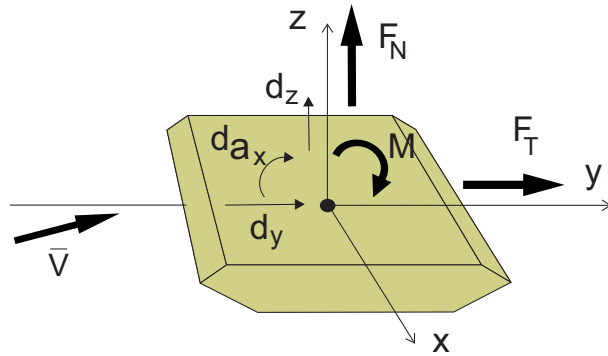
$$\vec{V} = \begin{Bmatrix} \bar{U}(P) \\ 0 \\ 0 \end{Bmatrix} + \begin{Bmatrix} u(P,t) \\ v(P,t) \\ w(P,t) \end{Bmatrix} \quad (1)$$

where  $\bar{U}(P)$  is the average wind speed (parallel to the x-axis of the coordinate system) and  $u(P,t)$ ,  $v(P,t)$  and  $w(P,t)$  the turbulent wind speed fluctuations along the x, y and z directions, respectively (see Fig. 1).

The random nature of turbulent wind speed fluctuations invokes the stochastic process theory as a well-adapted tool for representing such fluctuations. In this context, the parameters serving to characterize turbulent wind, along with its spatio-temporal variability, are: the standard deviations of turbulent speed fluctuations ( $\sigma_u, \sigma_v, \sigma_w$ ), turbulence scales, the spectral and interspectral power



□ **Figure 1**  
Components of turbulent wind speed



□ **Figure 2**  
Components of the force produced by turbulent wind

densities of each component, and the coherence coefficients. These parameters are all determined from wind speed measurements on the study site. Details on both the definition and estimation of these parameters are available in Biétry [11].

## Wind-generated forces on bridge decks

The presence of a structural body in airflow modifies locally both the flow trajectory and speed. These modifications depend on the shape of the body as well as on airspeed and wind turbulence level. The disturbances induced by the presence of the body in the flow also cause a pressure field to form around the body. Integration of this pressure field yields a torsor of aerodynamic forces, which is generally divided into three components: a so-called drag force  $F_T$  whose direction is parallel to that of the mean wind, a so-called lift force  $F_N$  perpendicular to the drag force, and a torsion moment  $M$  (see Fig. 2).

For a bridge deck situated in turbulent airflow, it is possible to approximate the forces generated by wind on the cross-section, by *summing the static forces corresponding to the mean wind, self-sustained forces and forces due to turbulence*. This sum is then justified by a first-order linearization of wind effects [7]. The aeolian forces can then be expressed as:

$$\{f(\vec{V}, P, t)\} = \overbrace{\{f^S(\bar{U}, P)\}}^{\text{Statiques}} + \overbrace{\{f^A(\bar{U}, \vec{d}, \dot{\vec{d}}, P, t)\}}^{\text{Aéroélastiques}} + \overbrace{\{f^T(\bar{U}, \vec{V}', P, t)\}}^{\text{Turbulence}} \quad (2)$$

where  ${}^t\{f(\vec{V}, t)\} = \{F_T(\vec{V}, t), F_N(\vec{V}, t), M(\vec{V}, t)\}$  represents the vector of forces generated by wind on the structure;  $\{f^S(\bar{U})\}$  the static force vector of the prevailing wind;  $\{f^A(\bar{U}, \vec{d}, \dot{\vec{d}})\}$  the aeroelastic (or self-sustained) force vector;  $\{f^T(\bar{U}, \vec{V}', t)\}$  the vector of forces generated by wind turbulence;  $\vec{V}'$  the vector containing turbulent wind speed fluctuations;  $\vec{d}'$  and  $\dot{\vec{d}}$  the structural displacement and speed vectors, respectively.

### Static forces

The components of static aerodynamic forces at point P along the deck can now be written as follows:

$$\{f^S(\bar{U}, P)\} = p\{C\} \quad (3)$$

with:  $p = \frac{1}{2}\rho B\bar{U}^2$ ,  ${}^t\{f^S(\bar{U}, P)\} = \{F_T^S(\bar{U}, P, t), F_N^S(\bar{U}, P, t), M^S(\bar{U}, P, t)\}$ ;  ${}^t\{C\} = \{C_T, C_N, BC_M\}$

where  $\rho$  is the mass density of air,  $B$  a characteristic section dimension (in general the width),  $C_T$ ,  $C_N$ , and  $C_M$  the aerodynamic coefficients of drag, lift and moment, which depend on the incident wind angle. These coefficients are measured during wind tunnel tests.

## Aeroelastic forces

In Equation (2), the terms associated with the turbulence incorporate both speed fluctuations and incident wind angle with respect to the deck at "rest", whereas aeroelastic terms are related to the aerodynamic forces produced by deck movement. These forces may be expressed over either the time or frequency domain.

The initial formulations that account for aeroelastic phenomena stem from the field of aeronautics and entail so-called *indicial functions*, which allow expressing the impact of a disturbance in the displacement signal on the aerodynamic force signal. The effect of displacement history, at time  $t$ , on the force signal value gets included by a convolution product. Formulations analogous to those developed for airfoils have been proposed for bridge decks by Bleich [1], Bisplinghoff [2], Lin [7] and Scanlan [12]. The fundamental difference in these models compared to those in aeronautics relates to being based on experimental parameters of the target cross-section. The vector containing the three aeroelastic force components at point P along the element takes the following form:

$$\{f^A(t,P)\} = [\chi]\{\dot{d}(t,P)\} + [C_0]\{d(t,P)\} + \int_0^t [C_1(t-\tau)]\{\dot{d}(\tau,P)\}d\tau + \int_0^t [C_2(t-\tau)]\{d(\tau,P)\}d\tau \quad (4)$$

with:  ${}^t\{f^A(t,P)\} = \{F_T^A(t,P), F_N^A(t,P), M^A(t,P)\}$

$${}^t\{d(t,P)\} = \{d_y(t,P) \quad d_z(t,P) \quad d_{\alpha_x}(t,P)\}, \quad {}^t\{\dot{d}(t,P)\} = \{\dot{d}_y(t,P) \quad \dot{d}_z(t,P) \quad \dot{d}_{\alpha_x}(t,P)\}$$

$$[\chi] = p \begin{bmatrix} \chi_{T_0,p} & \chi_{T_0,h} & \chi_{T_0,\alpha} \\ \chi_{N_0,p} & \chi_{N_0,h} & \chi_{N_0,\alpha} \\ B\chi_{M_0,p} & B\chi_{M_0,h} & B\chi_{M_0,\alpha} \end{bmatrix}, \quad [C_0] = p \begin{bmatrix} c_{0,Tp} & c_{0,Th} & c_{0,T\alpha} \\ c_{0,Np} & c_{0,Nh} & c_{0,N\alpha} \\ Bc_{0,Mp} & Bc_{0,Mh} & Bc_{0,M\alpha} \end{bmatrix}$$

$$[C_1(t-\tau)] = p \begin{bmatrix} c_{1,Tp}e^{c_{2,Tp}\beta(t-\tau)} & c_{1,Th}e^{c_{2,Th}\beta(t-\tau)} & c_{1,T\alpha}e^{c_{2,T\alpha}\beta(t-\tau)} \\ c_{1,Np}e^{c_{2,Np}\beta(t-\tau)} & c_{1,Nh}e^{c_{2,Nh}\beta(t-\tau)} & c_{1,N\alpha}e^{c_{2,N\alpha}\beta(t-\tau)} \\ Bc_{1,Mp}e^{c_{2,Mp}\beta(t-\tau)} & Bc_{1,Mh}e^{c_{2,Mh}\beta(t-\tau)} & Bc_{1,M\alpha}e^{c_{2,M\alpha}\beta(t-\tau)} \end{bmatrix}$$

$$[C_2(t-\tau)] = p \begin{bmatrix} c_{3,Tp}e^{c_{4,Tp}\beta(t-\tau)} & c_{3,Th}e^{c_{4,Th}\beta(t-\tau)} & c_{3,T\alpha}e^{c_{4,T\alpha}\beta(t-\tau)} \\ c_{3,Np}e^{c_{4,Np}\beta(t-\tau)} & c_{3,Nh}e^{c_{4,Nh}\beta(t-\tau)} & c_{3,N\alpha}e^{c_{4,N\alpha}\beta(t-\tau)} \\ Bc_{3,Mp}e^{c_{4,Mp}\beta(t-\tau)} & Bc_{3,Mh}e^{c_{4,Mh}\beta(t-\tau)} & Bc_{3,M\alpha}e^{c_{4,M\alpha}\beta(t-\tau)} \end{bmatrix}$$

where  $\beta = \bar{U}/B$ ; with  $d_j$  and  $\dot{d}_j$  ( $j = y,z,\alpha_x$ ) being the displacement and speed components at point P of the deck, respectively.  $\chi_{i_0,k}$  and  $c_{j,ik}$  ( $i = N,T,m; j = 0,\dots, 4; k = p,h,\alpha$ ) are the indicial function coefficients of the cross-section; these coefficients are determined either experimentally or from non-stationary coefficients of the cross-section [13].

In the frequency-based formulation, aeroelastic forces are expressed as functions of both the displacements and first derivative of displacements. These forces also depend on the real coefficients measured during a wind tunnel test on the section in oscillation; such coefficients in turn depend on wind speed and oscillation frequency [3]. The vector containing the three aeroelastic force components at any point on the deck axis can thus be written as follows:

$$\{f^A(\omega,P)\} = [a(\omega)]\{\dot{d}(\omega,P)\} + [b(\omega)]\{d(\omega,P)\} \quad (5)$$

which leads to stating:

$$[a(\omega)] = p \begin{bmatrix} P_1^*(K) & P_5^*(K) & BP_2^*(K) \\ H_5^*(K) & H_1^*(K) & BH_2^*(K) \\ BA_5^*(K) & BA_1^*(K) & B^2A_2^*(K) \end{bmatrix}; \quad [b(\omega)] = p \begin{bmatrix} P_4^*(K) & P_6^*(K) & BP_3^*(K) \\ H_6^*(K) & H_4^*(K) & BH_3^*(K) \\ BA_6^*(K) & BA_4^*(K) & B^2A_3^*(K) \end{bmatrix}$$

where  $\omega$  is the oscillation frequency;  $K = B\omega/\bar{U}$  the reduced frequency;  $H_i^*(K)$ ,  $P_i^*(K)$  and  $A_i^*(K)$  ( $i = 1, \dots, 6$ ) so-called non-stationary or Scanlan adimensional coefficients, measured during a wind tunnel test on a mobile model representing a deck cross-section.

### Forces due to turbulence

The hypothesis of a quasi-stationary position enables considering that *the instantaneous forces produced by turbulent wind on a deck segment are equal to those that would occur on this segment in permanent flow with the same speed and angle of incidence*. The approximations  $\alpha = \frac{w(t)}{\bar{U}}$  and  $C_i(\alpha) \approx C_i + \frac{dC_i}{d\alpha}$  ( $i = C, D$  or  $M$ ) serve to derive expressions for the terms due to turbulence:

$$\{f^T(t, P)\} = p\{C\} \frac{2u(t)}{\bar{U}} + p\left\{\frac{dC}{d\alpha}\right\} \frac{w(t)}{\bar{U}} \quad (6)$$

$$\text{with: } {}^t\{f^T(t, P)\} = \{F_T^T(t, P) \quad F_N^T(t, P) \quad M^T(t, P)\}; \quad {}^t\left\{\frac{dC}{d\alpha}\right\} = \left\{\frac{dC_T}{d\alpha}, \frac{dC_N}{d\alpha}, B \frac{dC_M}{d\alpha}\right\}$$

where  $\frac{dC_i}{d\alpha}$  ( $i = T, N, M$ ) are the derivatives of aerodynamic coefficients with respect to the incident wind angle.

It turns out that the quasi-stationary model provided by the previous set of equations is merely an approximation for evaluating the forces due to turbulence. Even for laminar flow, aerodynamic forces actually vary over time. The aerodynamic coefficients input into Equation (6) often consist of average values and are said to be stationary. In order to account for the non-stationary character of airflow, the aerodynamic forces must be corrected. A more precise representation of the problem [14] necessitates indicial functions analogous to those established for the definition of aeroelastic forces. This step leads to developing an expression for forces due to turbulence, i.e.:

$$\{f^T(t, P)\} = p\{C\} \int_0^t [\Psi(t-\tau)] \frac{2u(\tau)}{\bar{U}} d\tau + p\left\{\frac{dC}{d\alpha}\right\} \int_0^t [\Psi(t-\tau)] \frac{2w(\tau)}{\bar{U}} d\tau \quad (7)$$

$$\text{which then allows stating: } [\Psi(t-\tau)] = \begin{bmatrix} \Psi_{Tu}(t-\tau) & 0 & 0 \\ 0 & \Psi_{Nu}(t-\tau) & 0 \\ 0 & 0 & B\Psi_{Mu}(t-\tau) \end{bmatrix}$$

where  $\Psi_{ik}$  ( $i = N, T, M, k = u, w$ ) are the indicial functions.

### Finite element discretization

As indicated in the preceding sections, the mathematical models of wind effects on a bridge deck apply, on a section reference axis (e.g. the center of thrust), the resultant of pressures generated on the given section. This resultant force is expressed by means of three components (drag, lift and moment) distributed along the considered element. Within the scope of finite element discretization of a structure, the best-adapted type of model proves to be the *three-dimensional beam element*. In the local coordinate system of this element type, the displacement field of any point P along the element is defined as a function of nodal displacement vectors  $\{d_{nd}\}$ , via the interpolation matrix  $[N(s)]$ . This relation is written as follows:

$$\{d(P)\} = [N(s)]\{d_{nd}\} \quad (8)$$

The equivalent beam forces are yielded by the relation [15]:

$$\{f_{nd}^A\}_e^{Local} = \int_0^L {}^t[N(s)]\{f^A(s)\} ds \quad (9)$$

where  $\left\{f_{nd}^A\right\}_e^{Local}$  is the nodal force vector corresponding to element  $e$ , and  $L$  is the beam length.

As part of this study framework, the elements considered are 2-node, three-dimensional beam elements; the nodal force vector is thus of size 12. Expressions (8) and (9) serve to evaluate the aeolian forces at the extremity nodes of each beam element contained in the mesh representative of the structure. Building the nodal loading vector for the entire structure, by reliance upon the stiffness, mass and damping matrices, requires an element-by-element assembly process over the whole mesh. The vectors comprising the various aeolian force terms for an entire structure, as discretized by a mesh with "n" degrees of freedom, can then be expressed as follows:

■ **Aeroelastic forces** (time domain)

$$\{F^A(t)\} = [\tilde{\chi}]\{\dot{d}(t)\} + [\tilde{C}_0]\{d(t)\} + \int_0^t [\tilde{C}_1(t-\tau)]\{\dot{d}(\tau)\}d\tau + \int_0^t [\tilde{C}_2(t-\tau)]\{d(\tau)\}d\tau \quad (10)$$

where  $\{d(t)\}$  and  $\{\dot{d}(t)\}$  are respectively the displacement and nodal speed vectors (of size  $n$ ) of the mesh;  $[\tilde{\chi}]$ ,  $[\tilde{C}_0]$ ,  $[\tilde{C}_1(t-\tau)]$  and  $[\tilde{C}_2(t-\tau)]$  are the matrices (of size  $n \times n$ ) of indicial function coefficients for the entire structure; these matrices are formed by means of assembling the elementary matrices composed from relations (4), (8) and (9).

■ **Aeroelastic forces** (frequency domain)

$$\{F^A(\omega)\} = [A(\omega)]\{\dot{d}(\omega)\} + [B(\omega)]\{d(\omega)\} \quad (11)$$

where  $[A(\omega)]$  and  $[B(\omega)]$  are matrices (of size  $n \times n$ ) analogous to matrices  $[a(\omega)]$  and  $[b(\omega)]$  of Equation (5) and whose assembly process is analogous to that of the matrices in Equation (10).

■ **Forces due to turbulence** (time domain)

• *Quasi-stationary approach:*  $\{F^T(t)\} = [D]\{V'(t)\} \quad (12a)$

where  $\{V'(t)\}$  is the vector containing the three components of turbulent wind speed fluctuation for each node of the completed structure, and  $[D]$  a matrix that allows the transition between turbulent wind speed fluctuations and nodal forces generated on the entire structure. This matrix is also built by means of an assembly process that utilizes the elementary force formulation from Equation (6).

• *Indicial function approach:*  $\{F^T(t)\} = \int_0^t [D(t-\tau)]\{V'(\tau)\}d\tau \quad (12b)$

where  $[D(t-\tau)]$  is formed analogously to matrix  $[D]$ ; inside this matrix appears the indicial functions defined in Equation (7).

■ **Forces due to turbulence** (frequency domain)

• *Quasi-stationary approach:*  $\{F^T(\omega)\} = [D]\{V'(\omega)\} \quad (13a)$

• *Indicial function approach:*  $\{F^T(\omega)\} = [D(\omega)]\{V'(\omega)\} \quad (13b)$

where  $[D(\omega)]$  denotes the Fourier transform of  $[D(t)]$ ; inside this transform would appear terms of the type  $\Psi_{ik}(\omega)$  ( $i = N, T, M$ ,  $k = u, w$ ) obtained from the corresponding indicial functions defined in Equation (7).

Details of the formulation of these various aeolian force vectors may be found in reference [16].

## WIND RESPONSE STUDY

### Movement equations

The wind-induced vibrations on a flexible bridge, discretized by finite elements, are handled using a second-order differential system:

$$[M]\{\ddot{d}(t)\} + [C]\{\dot{d}(t)\} + [K]\{d(t)\} = \{F^A(\bar{U}, \dot{\bar{d}}, \bar{d}, t)\} + \{F^T(\bar{U}, \bar{V}', t)\} \quad (14)$$

in which  $[M]$ ,  $[C]$  and  $[K]$  are the mass, damping and stiffness matrices (size  $n \times n$ ) of the structure, respectively;  $n$  is the number of degrees of freedom of the system;  $\{d(t)\}$  is the nodal displacement vector;  $\{F^A(\bar{U}, \dot{\bar{d}}, \bar{d}, t)\}$  is the aeroelastic force vector (a function of the structure's mean wind speed,

displacements and oscillation speeds); and  $\{F^T(\bar{U}, \bar{V}', t)\}$  represents the vector of forces generated by turbulent wind.

The system in (14) can also be expressed over the frequency domain in the form:

$$(-\omega^2 [M] + i\omega [C] + [K])\{d(\omega)\} = \{F^A(\bar{U}, \dot{\bar{d}}, \bar{d}, \omega)\} + \{F^T(\bar{U}, \bar{V}', \omega)\} \quad (15)$$

Given relations (11) and (13b), it may be deduced that:

$$(-\omega^2 [M] + i\omega [C] + [K])\{d(\omega)\} = \overbrace{(i\omega [A(\bar{U}, \omega)] + [B(\bar{U}, \omega)])}^{\text{aéroélastique}} \{d(\omega)\} + \overbrace{[D(\omega)]\{V'(\omega)\}}^{\text{turbulence}} \quad (16)$$

The structural response may now be written in the basis  $[\Theta]$  formed by the first  $m$  eigenvectors of the undamped system:

$$\{d(\omega)\} = [\Theta]\{q(\omega)\} \quad (17)$$

where  $\{q(\omega)\}$  is the generalized coordinates vector.

By introducing (17) into (16) and by preliminarily multiplying the result by  ${}^t[\Theta]$ , the following may be derived:

$$(-\omega^2 [\hat{M}] + i\omega [\hat{C}] + [\hat{K}])\{q(\omega)\} = (i\omega [\hat{A}(\bar{U}, \omega)] + [\hat{B}(\bar{U}, \omega)])\{q(\omega)\} + {}^t[\Theta][D(\omega)]\{V'(\omega)\} \quad (18)$$

where  $[\hat{M}]$  et  $[\hat{K}]$  are the generalized diagonal mass and stiffness matrices;  $[\hat{C}]$  the generalized damping matrix, which is not necessarily diagonal;  $[\hat{A}(\bar{U}, \omega)]$  and  $[\hat{B}(\bar{U}, \omega)]$  the generalized aeroelastic damping and stiffness matrices. These matrices assume the form:

$$[\hat{M}] = {}^t[\Theta][M][\Theta]; \quad [\hat{C}] = {}^t[\Theta][C][\Theta]; \quad [\hat{K}] = {}^t[\Theta][K][\Theta] \quad (19a)$$

$$[\hat{A}(\bar{U}, \omega)] = {}^t[\Theta][A(\bar{U}, \omega)][\Theta]; \quad [\hat{B}(\bar{U}, \omega)] = {}^t[\Theta][B(\bar{U}, \omega)][\Theta] \quad (19b)$$

Use of the modal base enables reducing the differential system dimension by choosing an eigenvector subspace. Should the initial system be composed of  $n \times n$ -dimensioned matrices, the generalized system matrices will then be sized  $m \times m$  if  $[\Theta]$  comprises just  $m \leq n$  eigenmodes.

## Stability analysis

The coupled fluid-structure system, whose response has been described by Equation (18), becomes unstable when for a given wind speed  $\bar{U}$ , a frequency  $\omega$  exists capable of nullifying the determinant of the impedance matrix  $[G(\omega)]$ :

$$[G(\omega)] = \left[ -\omega^2 [\hat{M}] + i\omega \left( [\hat{C}] - [\hat{A}(\bar{U}, \omega)] \right) + \left( [\hat{K}] - [\hat{B}(\bar{U}, \omega)] \right) \right] \quad (20)$$

The wind speeds corresponding with this condition are called "critical flutter speeds". These speeds are determined by implementing the pK-F method, of the "fixed-point" type; this method has been inspired from the pK method used in aeronautics [17]. To proceed, solutions of the  $s = (\delta + i)\omega$  type are sought:

$$|[G(s)]| = \left| \left[ -s^2 [\hat{M}] + s \left( [\hat{C}] - [\hat{A}(\mathfrak{I}(s))] \right) + \left( [\hat{K}] - [\hat{B}(\mathfrak{I}(s))] \right) \right] \right| = 0 \quad (21)$$

where  $|\cdot|$  represents the determinant function, and  $\Re(s) = \delta\omega$  and  $\Im(s) = \omega$  are the real and imaginary parts of  $s$ , respectively.

In considering that the  $m$  frequencies  $\omega_{0,j}$  ( $j = 1, \dots, m$ ) of the undamped system have been computed, the method then consists of applying (for each frequency) the following iterative procedure, on the basis of an initial wind speed  $\bar{U}_0$  until reaching a final speed  $\bar{U}_f$ :

For a speed  $\bar{U}_k$  ( $k = 0, \dots, f$ ),

1. Computation of two initial values of  $s_j$ :

$$s_{j,1}(\bar{U}_k) = -0,01 \cdot \omega_{0,j} + i \cdot \omega_{0,j} \quad \text{et} \quad s_{j,2}(\bar{U}_k) = i \cdot \omega_{0,j}$$

2. Computation of the 18 non-stationary Scanlan coefficients corresponding to each frequency.

3. Computation of the determinant of  $[G(s)]$  corresponding to each value  $s_{j,1}(\bar{U}_k)$  and  $s_{j,2}(\bar{U}_k)$ .

4. The following value of  $s$  is then defined by use of a linear interpolation diagram:

$$s_{j,3}(\bar{U}_k) = \left( s_{j,2}(\bar{U}_k) \cdot \left[ \left| G(s_{j,1}) \right| \right] - s_{j,1}(\bar{U}_k) \cdot \left[ \left| G(s_{j,2}) \right| \right] \right) / \left( \left[ \left| G(s_{j,1}) \right| \right] - \left[ \left| G(s_{j,2}) \right| \right] \right)$$

5. Steps 3 and 4 are repeated until obtaining  $\left| \left[ G(s_{j,2}) \right] \right| < \text{tolerance 1}$ . Upon each new iteration  $s_{j,1}(\bar{U}_k) = s_{j,2}(\bar{U}_k)$  (preceding iteration) and  $s_{j,2}(\bar{U}_k) = s_{j,3}(\bar{U}_k)$ .

6. Once the step 5 test is verified, the *aeroelastically-modified* oscillatory response of the structure corresponding with speed  $\bar{U}$  has been identified. Moreover, if the condition:  $\left| \Re(s_{j,2}) \right| < \text{tolerance 2}$  is verified, flutter is encountered for angular frequency  $\left| \Im(s_{j,2}) \right|$  and speed  $\bar{U}_k$  constitutes a critical flutter speed.

Tolerances 1 and 2 are both convergence thresholds.

## Turbulence response computations

### Computation over the frequency domain

The first applications of random vibration theory to studying structures submitted to turbulent wind are attributed to Liepmann [14]; they focused on thin airfoils. Davenport [4] was the first to assimilate wind in the boundary atmospheric layer with turbulent flow and to generalize Liepmann's method for determining wind effects on suspension bridges.

This method considers the forces produced by turbulent wind on the structure like a random action (characterized by its spectral power density function) that induces vibrations to the structure. It then becomes possible to evaluate the standard deviation of the amplitude of the vibratory movements corresponding to each of the structure's eigenmodes. The primary stages of this approach are:

- characterization of the probabilistic nature of wind turbulence by the spectral power density (SPD) of turbulent speed fluctuations;
- probabilistic characterization of the forces produced by wind on the structure, by means of aerodynamic coefficients measured in a wind tunnel;
- computation of the structure's eigenmodes in order to determine its resonant response (system transfer function); and
- determination of statistical magnitudes characterizing the response (spectral power density of displacements and internal forces), using the previous data.

For a given average wind speed, Equation (18) yields the stochastic response of the structure in the following form:

$$\{q(\omega)\} = \left[ -\omega^2 [\hat{M}] + i\omega([\hat{C}] - [\hat{A}(\bar{U}, \omega)]) + ([\hat{K}] - [\hat{B}(\bar{U}, \omega)]) \right]^{-1} \cdot {}^t[\Theta][D(\omega)]\{V'(\omega)\} \quad (22)$$

$$\text{or moreover: } \{q(\omega)\} = [H(\omega)] \cdot {}^t[\Theta][D(\omega)]\{V'(\omega)\} \quad (23)$$

where  $[H(\omega)]$  is the *system transfer matrix*.

The spectral power density of the generalized coordinate is thereby obtained by multiplying the right-hand side of Equation (18) by its adjoint expression:

$$[S_{qq}(\omega)] = [H(\omega)] {}^t[\Theta][D(\omega)][S_{V'V'}(\omega)] {}^t[D(\omega)]^* [\Theta] {}^t[H(\omega)]^* \quad (24)$$

in which  $[S_{qq}(\omega)]$  is the spectral density matrix of the generalized coordinates,  $[S_{V'V'}(\omega)]$  the inter-spectral power density matrix of turbulent wind speed fluctuations, and "\*" the conjugation operator.

The interspectral density matrix of wind speeds is defined by:

$$[S_{V'V'}(\omega)] = \begin{bmatrix} S_{u_1u_1}(\omega) & S_{u_1v_1}(\omega) & S_{u_1w_1}(\omega) & & S_{u_1u_p}(\omega) & S_{u_1v_p}(\omega) & S_{u_1w_p}(\omega) \\ S_{v_1u_1}(\omega) & S_{v_1v_1}(\omega) & S_{v_1w_1}(\omega) & \cdots & S_{v_1u_p}(\omega) & S_{v_1v_p}(\omega) & S_{v_1w_p}(\omega) \\ S_{w_1u_1}(\omega) & S_{w_1v_1}(\omega) & S_{w_1w_1}(\omega) & & S_{w_1u_p}(\omega) & S_{w_1v_p}(\omega) & S_{w_1w_p}(\omega) \\ \vdots & & & \ddots & & \vdots & \\ S_{u_pu_1}(\omega) & S_{u_pv_1}(\omega) & S_{u_pw_1}(\omega) & & S_{u_pu_p}(\omega) & S_{u_pv_p}(\omega) & S_{u_pw_p}(\omega) \\ S_{v_pu_1}(\omega) & S_{v_pv_1}(\omega) & S_{v_pw_1}(\omega) & \cdots & S_{v_pu_p}(\omega) & S_{v_pv_p}(\omega) & S_{v_pw_p}(\omega) \\ S_{w_pu_1}(\omega) & S_{w_pv_1}(\omega) & S_{w_pw_1}(\omega) & & S_{w_pu_p}(\omega) & S_{w_pv_p}(\omega) & S_{w_pw_p}(\omega) \end{bmatrix} \quad (25)$$

where  $S_{\alpha_i\beta_j}(\omega)$  ( $\alpha, \beta = u, v, w$ ;  $i = 1, \dots, p$ ) is the interspectral power density between the range of wind fluctuations at various model nodes, with  $p$  being the number of nodes.

Within the product of expression (24),  $[D(\omega)] [S_{V'V'}(\omega)]^t [D(\omega)]^*$ , terms of the following type appear:

$$C_l \cdot C_m \cdot S_{jk}(\omega) \cdot \Psi_{lj}(\omega) \Psi_{mk}^*(\omega) + \dots \quad (26)$$

with  $l, m = T, N, M$ ;  $j, k = u, v, w$ ; the product  $\Psi_{ij}(\omega) \Psi_{km}^*(\omega)$  is known as the *aerodynamic admittance function*. The product (26) may be simplified by neglecting the interspectral density between different turbulent wind speed components, i.e.:

$$S_{jk}(\omega) = 0 \text{ pour } j \neq k \quad (27)$$

Another possible simplification consists of assuming that all aerodynamic admittance functions are equal. These two hypotheses thus allow factorizing the indicial function  $\Psi_{ij}(\omega)$  of matrix  $[D(\omega)]$ .

Lastly, the variance of the generalized coordinate is calculated using Equation (24) by:

$$[\sigma_{qq}^2] = \int_0^\infty [S_{qq}(n)] dn \quad (28)$$

or in Equation (17), the variance of nodal displacements may be evaluated by:

$$\sigma_{d_i}^2 = \sum_{k=1}^m \sum_{l=1}^m (\theta_k^i)_j \cdot (\theta_l^i)_j \int_0^\infty (S_{qq}(n))_{kl} dn \quad (29)$$

where  $j$  is the corresponding node number ( $j = 1, \dots, p$ ) and  $i$  the displacement component ( $i = y, z, \alpha$ ).

In practice, the extreme value of the response is essential for structural design. Consequently, the extreme value of the structure's displacements is set by:

$$\{\hat{d}\} = \{\bar{d}\} + g\{\sigma_d\} \quad (30)$$

where  $g$  is a peak factor whose value normally lies between 3.5 and 4.5 [4].

### Computation over the time domain

An alternative approach to spectral methods consists of first *simulating random turbulent wind speed signals* at the structure's nodes, then *integrating in the time domain the system movement equations*. This approach also serves to study structures exhibiting non-linear behaviour.

Within the general framework of a structure with *non-linear behaviour* with linear viscous damping, the system dynamics equation may be written in the form:

$$[M]\{\ddot{d}(t)\} + [C]\{\dot{d}(t)\} + \{P(t)\} = \{F^A(t)\} + \{F^T(t)\} \quad (31)$$

in which  $\{P(t)\}$  is the vector containing the forces developed by the structure at time  $t$  (these forces are a non-linear function of structural displacements),  $\{F^A(t)\}$  is the vector of aeroelastic forces, and  $\{F^T(t)\}$  denotes the vector of forces generated by turbulent wind on the structure at time  $t$ .

The vector of turbulent forces is expressed in the form of a Duhamel integral (12b):

$$\{F^T(t)\} = \int_0^t [D(t-\tau)] \{V'(\tau)\} d\tau$$

Inside the matrix,  $[D(t = \tau)]$  indicial functions of the type  $\Psi_{jk}$  ( $j = N, T, M$ ;  $k = u, w$ ) appear. Unfortunately, at present, no analytical or experimental formulation of these functions exists for bridge decks. As a result, for the temporal approach, the hypothesis of a quasi-stationary position has been adopted (2a), which then implies:

$$\{F^T(t)\} = [D] \{V'(t)\}$$

By applying the *modified Newton-Raphson* method to analyze non-linear systems [18], Equation (31) may be rewritten as follows:

$$[M] \{\dot{d}(t + \Delta t)\}^{(k)} + [C] \{d(t + \Delta t)\}^{(k)} + [{}^{tg}K] \{\Delta d\}^{(k)} + \{P(t + \Delta t)\}^{(k-1)} = \{F^A(t + \Delta t)\}^{(k-1)} + [D] \{V'(t + \Delta t)\} \quad (32)$$

$$\text{with: } \{\Delta d\}^{(k)} = \{d(t + \Delta t)\}^{(k)} - \{d(t + \Delta t)\}^{(k-1)} \quad (33)$$

$$\{P(t + \Delta t)\}^{(k)} = \{P(t + \Delta t)\}^{(k-1)} + [{}^{tg}K] \{\Delta d\}^{(k)} \quad (34)$$

$[{}^{tg}K]$  is the *tangent stiffness* matrix of the structure at time  $t$ , and  $k$  the corresponding iteration number ( $k = 1, 2, 3, \dots$ ). The initial values of iterations  $k$  are provided by:

$$\{d(t + \Delta t)\}^{(0)} = \{d(t)\}, \{P(t + \Delta t)\}^{(0)} = \{P(t)\}, \{F^A(t + \Delta t)\}^{(0)} = \{F^A(t)\} \quad (35)$$

The temporal integration of movement equations may be conducted in an approximate fashion with Newmark's method. The following hypotheses, with respect to displacements and speeds at time  $t + \Delta t$ , can then be incorporated:

$$\{\dot{d}(t + \Delta t)\}^{(k)} = -\{\dot{d}(t)\} + \frac{2}{\Delta t} (\{d(t + \Delta t)\}^{(k-1)} - \{d(t)\} + \{\Delta d(t)\}^{(k)}) \quad (36)$$

$$\{\ddot{d}(t + \Delta t)\}^{(k)} = \frac{4}{\Delta t^2} (\{d(t + \Delta t)\}^{(k-1)} - \{d(t)\} + \{\Delta d(t)\}^{(k)}) - \frac{4}{\Delta t} (\{\dot{d}(t)\} - \{\ddot{d}(t)\}) \quad (37)$$

Substituting Equations (36) and (37) into (32) yields:

$$[\bar{K}] \{\Delta d\}^{(k)} = \{\Delta R\}^{(k-1)} \quad (38)$$

$$\text{with: } \{\Delta R\}^{(k-1)} = \{F^A(t + \Delta t)\}^{(k-1)} + [D] \{V'(t + \Delta t)\} - \{P(t + \Delta t)\}^{(k-1)} - [M] \{g_M\} - [C] \{g_C\} \quad (39)$$

$$[\bar{K}] = \left[ [M] \frac{4}{\Delta t^2} + [C] \frac{2}{\Delta t} + [{}^{tg}K] \right]; \{g_M\} = \left[ \frac{4}{\Delta t^2} (\{d(t + \Delta t)\}^{(k-1)} - \{d(t)\}) - \frac{4}{\Delta t} (\{\dot{d}(t)\} - \{\ddot{d}(t)\}) \right]$$

$$\{g_C\} = \left[ \frac{2}{\Delta t} (\{d(t + \Delta t)\}^{(k-1)} - \{d(t)\}) - \{\dot{d}(t)\} \right]$$

Equation (38) is the method's fundamental expression. Within each time step, it is thus necessary to start by computing the "residual" vector that complies with Equation (39) and then the displacement increment vector  $\{\Delta d\}^{(k)}$  from the expression in (33). The new values of  $\{d(t + \Delta t)\}^{(k)}$  and  $\{\dot{d}(t + \Delta t)\}^{(k)}$  are computed next on the basis of Equations (36) and (37), respectively. This sequence leads to a new value of the residual; iterations ( $k = 1, 2, 3, \dots$ ) then get repeated until the value of  $\{\Delta d\}^{(k)}$  is rendered small enough.

## APPLICATION TO THE VASCO DE GAMA BRIDGE

The theoretical developments set forth above were implemented in the CESAR-LCPC<sup>®</sup> software package and applied to studying the wind response of a specific structure: the Vasco de Gama Bridge, over the Tagus River in Lisbon: a cable-stayed bridge with a central span measuring 420 m

for an 830-m total length. The deck is 30.9 m wide and formed by one reinforced concrete slab and two lateral prestressed beams 2.60 m high. The aeolian data of the project site are listed in Table I. Table II and Figure 3 show the aerodynamic and aeroelastic characteristics of the deck cross-section.

The selected Vasco de Gama Bridge model used in this study was devised by the SETRA Engineering Agency during structural design studies conducted using the SYSTUS finite element code. For the present study, this model was input into the CESAR-LCPC program; it contains 754 nodes and 1,325 three-dimensional beam elements. Figure 4 displays the bridge model mesh. The first eight eigenfrequencies of the bridge computed with CESAR-LCPC are provided in Table III. All modes are damped using a structural damping coefficient of 0.57%.

Figure 5 depicts the variation in modal damping vs. wind speed at deck level. The stability loss due to flutter (zero damping condition) arises for the first and second torsion modes at wind speeds of 84.6 m/sec and 111.5 m/sec, respectively. The first critical flutter speed for the complete bridge model may be compared to that obtained from wind tunnel measurements on a taut-strip model test. The instability speed, as measured in a wind tunnel, corresponds to 89.2 m/sec on a full-scale structure. Despite the differences between mechanical models and between turbulence characteristics in a wind tunnel and on site, the two critical speeds are relatively similar.

Turbulence response has been evaluated for a computation speed corresponding to 39.3 m/sec at deck level (52 m above ground). Only the first ten vibration modes were considered for this computation. Turbulence has been modeled to conform with data from Table I. Figure 6 presents the variation in standard deviation of vertical displacements along the bridge deck.

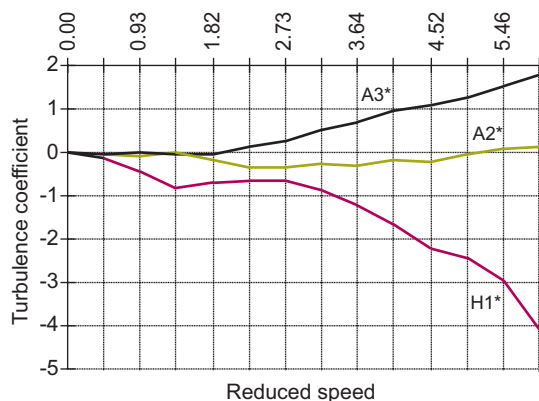
**TABLE I**  
Turbulence characteristics of the study site

Roughness: $z_0^* = 0.005$ mm; average speed at 10 m: $\bar{U}_{10} = 32.3$ m/sec
Turbulence intensities: $I_u = 0.11$ ; $I_v = 0.11$ ; $I_w = 0.07$
Longitudinal scales: $L_y^u = 185$ m; $L_y^v = 60$ m; $L_y^w = 30$ m
Transverse scales: $L_x^u = 75$ m; $L_x^v = 90$ m; $L_x^w = 30$ m
Vertical scales: $L_z^u = 40$ m; $L_z^v = 30$ m; $L_z^w = 20$ m
Lateral coherence: $C_x^u = 11$ ; $C_x^v = 4,5$ ; $C_x^w = 12$
Vertical coherence: $C_z^u = 11$ ; $C_z^v = 4,5$ ; $C_z^w = 12$

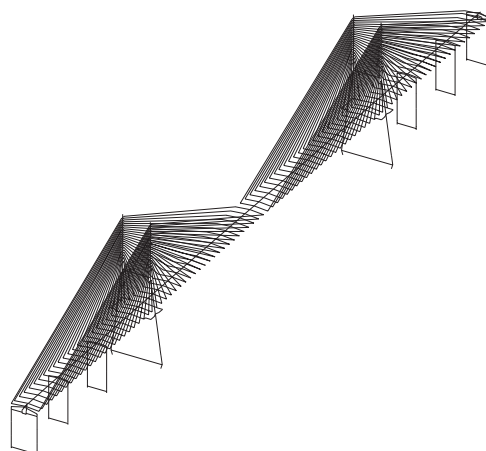
**TABLE II**  
Aerodynamic and aeroelastic characteristics of the bridge deck

Aerodynamic data (extracted from [19])	Indicial function coefficients (extracted from [13])	
$C_T(0) = 0.144$		
$C_N(0) = -0.0337$	$\chi_{N_{0,h}} = -14,6688$	$\chi_{M_{0,\alpha}} = 0,2624$
$C_M(0) = 0.015$	$c_{0,Nh} = 7,2204$	$c_{0,M\alpha} = 0,5594$
$dC_T(0)/d\alpha = 0,086$	$c_{1,Nh} = -6,3091$	$c_{1,M\alpha} = -39,5736$
$dC_N(0)/d\alpha = 5,960$	$c_{2,Nh} = -1,5931$	$c_{2,M\alpha} = -1,7175$
$dC_M(0)/d\alpha = 1,060$	$c_{3,Nh} = -7,0520$	$c_{3,M\alpha} = -42,7244$
	$c_{4,Nh} = -0,8210$	$c_{4,M\alpha} = -1,9910$

As for modelling bridge deck aeroelastic forces, the indicial function coefficients from Table II were used. "Synthetic" signals of *spatially-correlated* turbulent wind speeds were derived along the structure [20]. Figure 7 shows the variations in both vertical and horizontal wind speed components along the deck at time  $t = 10$  sec for one of these wind simulations.



□ **Figure 3**  
Aeroelastic coefficients of the deck cross-section  
(extracted from [19])



□ **Figure 4**  
Finite element mesh of the Vasco de Gama Bridge

**TABLE III**  
Eigenfrequencies of the Vasco de Gama Bridge model

Mode	Frequency (Hz)	Type
1	0.165	Longitudinal
2	0.329	Vertical bending
3	0.360	Sway
4	0.439	Vertical bending
5	0.494	Torsion
6	0.613	Vertical bending
7	0.638	Torsion
8	0.760	Vertical bending

In order to integrate movement equations, the time step was set at 2.5 ms and the simulation period at 40 sec. Figure 7 displays the variation in standard deviation of vertical displacements along the deck for various simulations of turbulent wind speeds. The estimation of these standard deviations is also given for five wind simulations, in addition to the results obtained from the frequency method (without aerodynamic admittance). It may be observed that results computed using the temporal method slightly overestimate those resulting from frequency computations. These differences are related primarily to the estimation of indicial function coefficients based on Scanlan coefficients.

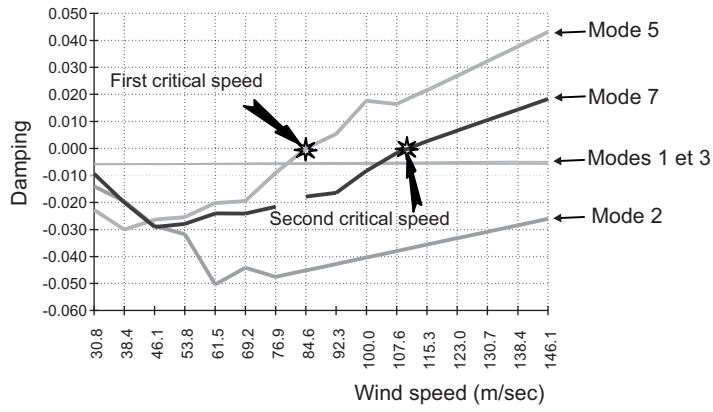


Figure 5  
Computation of critical flutter speeds

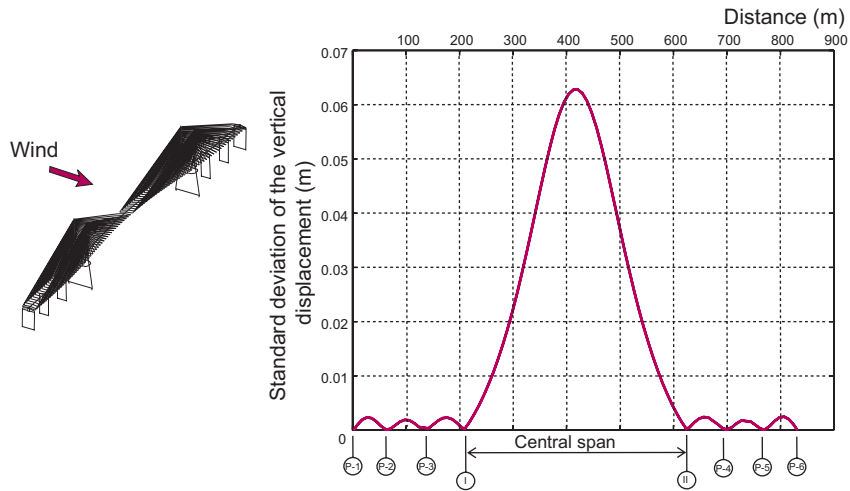


Figure 6  
Standard deviation of vertical displacements on the deck axis

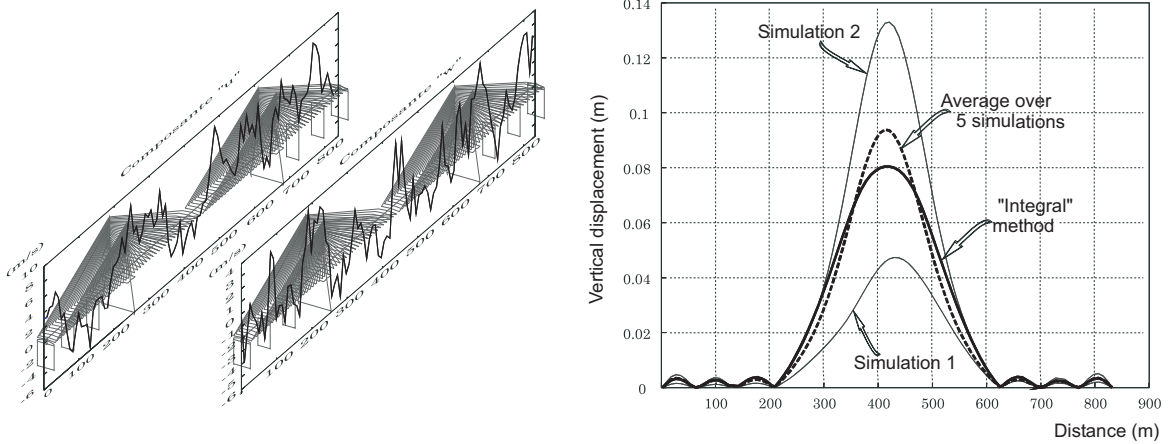


Figure 7  
Variation in vertical and horizontal wind components, and variation in the standard deviation of vertical displacements on the deck axis

## CONCLUSION

The study presented herein has proposed a general formulation for evaluating the response of bridges sensitive to wind effects on frequency and time domain. Conducted within the scope of a finite element-driven formalism, the approach adopted has relied upon incorporating aeroelastic effects into turbulence response computations. These effects represent the interaction between air and moving structure; they serve to highlight the oscillation frequency dependence of the structure's damping and stiffness terms. The stability analysis of the coupled "fluid-structure" system allows determining the speeds at which a risk of flutter appears. A method for identifying these critical speeds has moreover been proposed. Both the stability analysis and turbulence response computation methods were numerically implemented within a specific module of the CESAR-LCPC finite element computation code. These developments were validated by means of comparison with experimental data on an aeroelastic model. This module was then applied to compute full structures, for which a sampling of results has also been included.

## REFERENCES

- [1] BLEICH F., Dynamic instability of truss-stiffened suspension bridges under wind action, *Proc., ASCE*, vol. 74, **8**, 1948, pp. 1269-1314.
- [2] BISPLINGHOFF R.L., ASHLEY H., *Principles of Aeroelasticity*, John Wiley and Sons, États-Unis, 1962.
- [3] SCANLAN R.H., TOMKO J.J., Airfoil and bridge flutter derivatives, *Journal of Engineering Mechanics*, ASCE, vol. 109, **2**, 1971, pp. 586-603.
- [4] DAVENPORT, A.G., The buffeting response of a suspension bridge by storm winds, *Journal of the Structural Division*, ASCE, 88(33), 1962, pp. 233-268.
- [5] BIÉTRI J., GRILLAUD G., Wind studies for the Normandie bridge, *Actes de la conférence de l'AFPC sur les ponts suspendus et à haubans*, Deauville, France, vol. 2, 1994, pp. 29-44.
- [6] JAIN A., JONES N.P., SCANLAN R.H., Coupled flutter and buffeting analysis of long-span bridges, *Journal of Structural Engineering*, ASCE, vol. 122, **7**, 1996, pp. 717-725.
- [7] LIN Y.K., YANG J.N., Multimode bridge response to wind excitations, *Journal of Engineering Mechanics Division*, ASCE, vol. 100, **4**, 1983, pp. 657-672.
- [8] SCANLAN R.H., Problematics in formulation of wind-force models for bridge decks, *Journal of Engineering Mechanics*, ASCE, vol. 119, **7**, 1993, pp. 1353-1375.
- [9] ARZUMANIDIS S.G., BIENIEK M.P., Finite element analysis of suspension bridges, *Computers & Structures*, vol. 21, **6**, 1985, pp. 1237-1253.
- [10] BELIVEAU J.G., VAICAITIS R., SHINOZUKA M., Motion of suspension bridge subject to wind loads, *Journal of the Structural Division*, ASCE, vol. 103, **ST6**, 1977, pp. 1189-1205.
- [11] CRÉMONA C., Éd., *Comportement au vent des ponts*, AFGC, Presses de l'ENPC, Paris, France, 2002.
- [12] SCANLAN R.H., BELIVEAU J.G. BUDLONG K.S., Indicial aerodynamic functions for bridge decks, *Journal of Engineering Mechanics Division*, ASCE, vol. 100, **4**, 1974, pp. 657-672.
- [13] LEFORT M.-A., *Étude de la stabilité aéroélastique des ponts à haubans : approche numérique*, Université Blaise Pascal, Clermont-Ferrand II, France, 1998.
- [14] DOWEL E.H. (Ed.), CRAWLEY E.F., CURTISS H.C., PETERS D.A., SCANLAN R.H., SISTO F., *A Modern Course in Aeroelasticity*, Ed. Kluwer, USA, 1995.
- [15] IMBERT J.-F., *Analyse des structures par éléments finis*, éd. CEPADUES, 1979.
- [16] PATRON A., *Modélisation numérique de la tenue au vent des ponts souples*, Thèse de l'ENPC, 1998.
- [17] NAMINI A., ALBRECHT P., BOSCH H. (1992), Finite element-based flutter analysis of cable-suspended bridges, *Journal of Structural Engineering*, ASCE, vol. 118, **6**, 1992, pp. 1509-1526.
- [18] BATHE K.J., *Finite element procedures in engineering analysis*, Prentice-Hall Inc., New Jersey, États-Unis, 1996.
- [19] GRILLAUD G. et al., Wind action on the Vasco da Gama cable stayed bridge, *2nd European Conference on Wind Engineering*, G. Solari Ed., SGE Editoriali, Italie, 1997, pp. 1451-1456.
- [20] GUILLIN A., CRÉMONA C., *Développement d'algorithmes de simulation de champs de vitesse de vent*, Presses du LCPC, 1998.